MATHEMATICS AND COMPUTATIONAL SCIENCES

Vol 5(1), 2024, pp:43-54

DOI:10.30511/MCS.2024.2013489.1142

ISSN:2717-2708

http://mcs.qut.ac.ir/

Qom University of Technology

Applying Haar-Sinc spectral method for solving time-fractional Burger equation

Ali Pirkhedri [1]

Abstract: Haar-Sinc spectral method is used for the numerical approximation of time fractional Burgers' equations with variable and constant coefficients. The main idea in this method is using a linear discretization of time and space by combination of Haar and Sinc functions, respectively. While implementing the method, the operational matrices of the fractional integral of the fractional Haar functions are made, and by using them, an algebraic equation is obtained. Then, using the collocation method, the algebraic equation is converted into a system of equations, and after solving the system with Maple software, the numerical results of the problem is obtained. The accuracy and speed of the proposed algorithm are tested by obtaining L^{∞}, L^2 error and the convergence rate ($C-rate=\frac{\log(\frac{e_{n_1,k}}{e_{n_2,k}})}{\log(\frac{h1}{h2})}$).

Keywords: Time-fractional; Burgers' equation; Haar functions; Sinc functions; Collocation method; L^2-error; L^{∞}-error; Convergence rate
2020 Mathematics Subject Classification: 65M70; 35R11; 35E15; 26A33
Receive: 14 October 2023, **Accepted:** 24 March 2024

1 Introduction

In many real problems, modeling using the concept of derivative and integral of fractional order gives a more appropriate description of the facts of the problem compared to integer order of derivatives and integrals. Therefore, with the increase of applications and modeling based on fractional calculations, the necessity of developing analytical and numerical methods for this category of equations becomes more obvious and visible. Usually, obtaining accurate and analytical solutions for fractional order equations is not a simple task and in many cases, the exact answers are finally written in terms of an infinite series, which is expensive to calculate. Therefore, the need to develop computational methods with high accuracy and speed for solving fractional equations is justifiable [21]. Burgers' equation is one of the most important and basic equations with many scientific and practical applications. This equation is a good model for the study of gas dynamics, fluid movement, disturbance and turbulence in hydrodynamics, wave processes, boundary layers, diffusion in porous media and the speed of sediment particles falling in stagnant fluid.This equation is a simplified model of the Navier-Stokes equation that preserves many of the properties of this equation [2, 11] . By replacing the first-order time derivative with a fractional one, the time fractional

[1]Corresponding author: Department of Computer Engineering , Islamic Azad University, Marivan Branch, Marivan, Iran, alipirkhedri@gmail.com

Burgers' equation can be derived from the classical Burgers' equation in the following manner[6]:

$$\frac{\partial^\kappa \Phi(x,t)}{\partial t^\kappa} + \Phi(x,t)\frac{\partial \Phi(x,t)}{\partial x} - \gamma \frac{\partial^2 \Phi(x,t)}{\partial x^2} = Q(x,t), \quad 0 < x < 1, \quad 0 < t \leq 1, \tag{1.1}$$

with initial conditions

$$\Phi(x,0) = r(x), \quad 0 < x < 1, \tag{1.2}$$

and boundary conditions

$$\Phi(0,t) = f1(t), \Phi(1,t) = f2(t), \quad 0 < t < 1, \tag{1.3}$$

where the functions $Q(x,t), r(x), f1(t)$ and $f2(t)$ are known continuous functions,γ is viscosity parameter and $0 < \kappa \leq 1$ is Caputo fractional order derivative. The nonlinear time fractional Burgers' equation is difficult to solve and there are many numerical and analytical solutions such as, trigonometric tension B-spline collocation [23], the fractional reduced differential transform method [25], finite difference and Fibonacci collocation method [12], Lucas polynomials coupled with finite difference method [1], Fourier spectral approximation [4], the Crank-Nicolson approximation [17], weighted meshless spectral method[10], unified finite difference Chebyshev wavelet method [18], cubic spline based differential quadrature method[7], L1/LDG method [14], orthonormal shifted discrete Legendre polynomials [8] and expansion method by the Cole-Hopf transformation[27]. In certain cases, analytical solution of this equation is very difficult and even impossible. Therefore, according to the importance of the subject and in order to help the scientific and industrial communities, in this paper we will obtain the numerical solution of this equation and check the stability and convergence rate of the algorithm. For this purpose, we first introduce the fractional derivative and the Caputo derivative and express the characteristics of fractional derivatives and the relationships between them, and then we consider the properties of orthogonal Haar and Sinc functions. Then, using the Haar operational matrix of fractional order integration, we expand the time part of the equation in terms of Haar functions and the space part in terms of orthogonal Sinc functions. Then, by using the spectral collocation method the residual function have been obtained and the numerical solution of the equation is converted into the solution of an algebraic equation system which can be solved by Maple software. Finally, by presenting two examples and its numerical results by tables and graphs, we compare the numerical results with previous published works and we show that the order of convergence of the proposed method is exponential and is faster and more accurate than other methods.

2 Caputo's fractional order derivative

In this section, we would like to briefly explain the concept of the Caputo's fractional order derivative ($\kappa > 0$) [21, 13, 26]. Suppose s is the smallest integer greater than κ, then the derivative of Caputo's fractional order can be defined as:

$${}_d^C D_t^\kappa \Phi(x,t) = \begin{cases} I_t^{s-\kappa} D_t^s \Phi(x,t), & s-1 < \kappa < s, \\ D_t^s \Phi(x,t), & \kappa = s, s \in N, \end{cases} \tag{2.1}$$

where

$$I_t^\kappa \Phi(x,t) = \frac{1}{\Gamma(\kappa)} \int_d^t (t-\rho)^{\kappa-1} \Phi(x,\rho) d\rho, \quad t, \kappa > 0. \tag{2.2}$$

Also the following properties for fractional integral and derivatives can be listed as follows:

$$I_t^\kappa (t^\beta) = \frac{\Gamma(\beta+1)}{\Gamma(\kappa+\beta+1)} t^{\kappa+\beta},$$
$$I_t^\kappa (x^\beta t^\gamma) = x^\beta I_t^\kappa (t^\gamma),$$

$$D_t^{\kappa}(a\Phi(x,t)+bS(x,t))=aD_t^{\kappa}\Phi(x,t)+bD_t^{\kappa}S(x,t). \tag{2.3}$$

The left and right Caputo fractional derivatives of order $\kappa>0$ of a function $\Phi(x,t)$ where $d<t<e$ are defined by [26] :

$${}_d^{\mathcal{C}}D_t^{\kappa}\Phi(x,t)={}_dD_t^{\kappa}\left(\Phi(x,t)-\Phi(x,d)\right), \tag{2.4}$$

and

$${}_t^{\mathcal{C}}D_e^{\kappa}\Phi(x,t)={}_tD_e^{\kappa}\left(\Phi(x,t)-\Phi(x,e)\right), \tag{2.5}$$

respectively, where ${}_dD_t^{\kappa}\left(\Phi(x,t)\right)$ and ${}_tD_e^{\kappa}\left(\Phi(x,t)\right)$ denote the left and right Riemann–Liouville fractional derivative of order κ , that is,

$${}_dD_t^{\kappa}\left(\Phi(x,t)\right)=\frac{1}{\Gamma(1-\kappa)}\frac{d}{dt}\int_d^t(t-\rho)^{-\kappa}\Phi(x,\rho)d\rho, \tag{2.6}$$

$${}_tD_e^{\kappa}\left(\Phi(x,t)\right)=\frac{-1}{\Gamma(1-\kappa)}\frac{d}{dt}\int_t^e(\rho-t)^{-\kappa}\Phi(x,\rho)d\rho. \tag{2.7}$$

2.1 Rationalized Haar Functions

In this part, we would like to examine several formulas in relation to rationalized Haarfunctions and its fractional order of integral and derivative. Full explanations are available in references [3, 22, 15, 9]. More generally, we define the RH functions over the interval $[a,b)$ as:

$$R_v(t)=\begin{cases}1, & p_1\le t<p_{\frac{1}{2}}\\ -1, & p_{\frac{1}{2}}\le t<p_0,\\ 0, & \text{otherwise},\end{cases} \tag{2.8}$$

$$R_0(t)=1,\quad p_q=a+\left(\frac{n-q}{2^m}\right)(b-a),\quad q=0,\frac{1}{2},1,\quad a,b>0. \tag{2.9}$$

$$v=2^m+n-1,\quad m=0,1,2,...,\quad n=1,2,3,...,2^m. \tag{2.10}$$

Due to the completeness of Haar functions in domain (a,b), any arbitrary function $y(t)$ can be expanded with arbitrary precision:

$$y(t)\simeq\sum_{v=0}^{k-1}x_vR_v(t)=X^T\gamma_k(t),\quad k=2^{s+1},\quad s=0,1,2,.... \tag{2.11}$$

Also, this expansion can be expressed in the form of the following matrix forms:

$$X=\left[x_0,\quad x_1,\quad \ldots,\quad x_{k-1}\right]^T, \tag{2.12}$$

$$\gamma_k(t)=\left[R_0(t),\quad R_1(t),\quad \ldots,\quad R_{k-1}(t)\right]^T. \tag{2.13}$$

Also, the integral of Haar functions can be calculated as the following matrix form:

$$\int_0^t\gamma_k(s)ds\simeq L_{k\times k}\gamma_k(t), \tag{2.14}$$

$$L_{k\times k}=\frac{b}{2k}\begin{bmatrix}2kL_{(\frac{k}{2})\times(\frac{k}{2})} & -\Omega_{(\frac{k}{2})\times(\frac{k}{2})}\\ \Omega^{-1}_{(\frac{k}{2})\times(\frac{k}{2})} & 0\end{bmatrix}_{k\times k}, \tag{2.15}$$

$$\Omega_{k\times k} = \left[\gamma_k(\tfrac{1}{2k}), \gamma_k(\tfrac{3}{2k}), \ldots, \gamma_k(\tfrac{2k-1}{2k})\right]_{1\times k}, \tag{2.16}$$

where $\Omega_1 = [1]$, $L_1 = [\frac{1}{2}]$.
Also, the fractional order integral of Haar functions $(I_t^\kappa \gamma_k)(t)$ can be calculated as the following matrix form:

$$(I_t^\kappa \gamma_k)(t) = L_{k\times k}^\kappa \gamma_k(t), \tag{2.17}$$

$$L_{k\times k}^\kappa = \Omega_{k\times k} T^\kappa \Omega_{k\times k}^{-1}, \tag{2.18}$$

$$T^\kappa = \frac{1}{k^\kappa}\frac{1}{\Gamma(\kappa+2)}\begin{bmatrix} 1 & \omega_1 & \omega_2 & \ldots & \omega_{k-1} \\ 0 & 1 & \omega_1 & \ldots & \omega_{k-2} \\ 0 & 0 & 1 & \ldots & \omega_{k-3} \\ & & & \ddots & \vdots \\ 0 & 0 & 0 & 0 & 1 \end{bmatrix}_{k\times k}, \tag{2.19}$$

$$\omega_r = (r+1)^{\kappa+1} - 2r^{\kappa+1} + (r-1)^{\kappa+1}. \tag{2.20}$$

2.2 Sinc functions

The general characteristics of the Sinc function have been examined in references [20, 16] and in this section we briefly explain some of the features of this function. This function is defined as follows in the infinite interval:

$$Sinc(x) = \begin{cases} \frac{\sin(\pi x)}{\pi x} & x \neq 0 \\ 1 & x = 0 \end{cases}. \tag{2.21}$$

The set of Sinc functions for the constant parameter h and different values of m form a complete orthogonal set in the Hilbert space and any arbitrary function f can be expanded in terms of these functions:

$$S_m(h,x) \equiv Sinc(\frac{x-mh}{h}) = \begin{cases} \frac{\sin(\frac{\pi}{h}(x-mh))}{\frac{\pi}{h}(x-mh)} & x \neq mh, \\ 1 & x = mh, \end{cases} \tag{2.22}$$

$$S_m(h,jh) = \delta_{mj} = \begin{cases} 1 & j = m, \\ 0 & j \neq m, \end{cases} \tag{2.23}$$

$$f_{m,h}(x) = \sum_{m=-\infty}^{\infty} f(mh) Sinc(\frac{x-mh}{h}). \tag{2.24}$$

To approximate the functions that are in the $(0,1)$ range, we can use the translating with the $\psi(x)$ function as follows:

$$\psi(x) = \ln(\frac{x}{1-x}), \tag{2.25}$$

$$S_m(x) \equiv S(m,h)\circ\psi(x) = Sinc(\frac{\psi(x)-mh}{h}). \tag{2.26}$$

According to the above equations, the set of collocation points x_m is defined as:

$$x_m = \psi^{-1}(mh) = \frac{e^{mh}}{1+e^{mh}}, m = 0, \pm1, \pm2, ... \tag{2.27}$$

Also, the value of the Sinc function and the first and second order derivatives at the collocation points x_m are defined as [19]:

$$\delta_{m,j}^{(0)} = [S(m,h)\circ\psi(x)]|_{\,x=x_j} = \begin{cases} 1 & m = j, \\ 0 & m \neq j, \end{cases} \tag{2.28}$$

$$\delta^{(1)}_{m,j} = \frac{d}{d\psi}[S(m,h)\circ\psi(x)]|_{\ x=x_j} = \frac{1}{h}\begin{cases}0 & m=j,\\ \frac{(-1)^{j-m}}{j-m} & m\neq j,\end{cases} \tag{2.29}$$

$$\delta^{(2)}_{m,j} = \frac{d^2}{d\psi^2}[S(m,h)\circ\psi(x)]|_{\ x=x_j} = \frac{1}{h^2}\begin{cases}\frac{-\pi^2}{3} & m=j,\\ \frac{-2(-1)^{j-m}}{(j-m)^2} & m\neq j.\end{cases} \tag{2.30}$$

3 Error and Convergence rate

According to the theorems that have been proven in the references[5, 24], the approximation error of Haar and Sinc functions is as follows.

3.1 Rationalized Haar functions

If $D^{\kappa}_{\star}y_q(t)$ is an approximation with q resolution of $D^{\kappa}_{\star}y(t)$ function, then:

$$\|D^{\kappa}_{\star}y(t) - D^{\kappa}_{\star}y_q(t)\|_E \leq \frac{1}{q^{s-\kappa}}\frac{B}{\Gamma(s-\kappa).(s-\kappa)}\frac{1}{\sqrt{s-2^{2(s-\kappa)}}}, \tag{3.1}$$

$$D^{\kappa}_{\star}y_q(t) = \sum_{i=0}^{q-1} c_i R_i(t), \tag{3.2}$$

and,

$$\|y(t)\|_E = \left(\int_0^1 y^2(t)dt\right)^{\frac{1}{2}}. \tag{3.3}$$

3.2 Sinc functions

If there are constants $C>0$, $\alpha>0$ and $0<d\leq\frac{\pi}{2}$ such that $|y(x)|\leq Ce^{-\alpha|\psi(x)|}$ by choosing $h=\sqrt{\frac{\pi d}{\alpha N}}\leq \frac{2\pi d}{\ln(2)}$, then the estimation error is:

$$\left|y(x) - \sum_{k=-N}^{N} y(kh)S(k,h)\circ\psi(x)\right| \leq K\sqrt{N}e^{(-\sqrt{\pi d\alpha N})},$$

where K depends only on d,α and y.

4 Haar-Sinc collocation method

To approximate the unknown function $\Phi(x,t)$ and in order to use the operational matrix of Haar's fractional integral, we first expand $\frac{\partial\Phi_(x,t)}{\partial t}$ in terms of Haar and Sinc functions as:

$$\frac{\partial\Phi_{n,k}(x,t)}{\partial t} = \sum_{i=-n}^{n}\sum_{j=0}^{k-1} c_{ij}S_i(x)R_j(t). \tag{4.1}$$

Then, by applying the operational matrix of the fractional integral of Haar functions and using the value of the Sinc functions and its derivatives at the collocational points x_m, the following equations are established:

$$\Phi_{n,k}(x_m,t) = r(x_m) + \sum_{j=0}^{k-1}\sum_{l=0}^{k-1} c_{ml} L_{lj} R_j(t) \tag{4.2}$$

$$\frac{\partial^\kappa \Phi_{n,k}(x_m,t)}{\partial t^\kappa} = \left(D_t^\kappa r(x)\right)_{x_m} + \sum_{j=0}^{k-1}\sum_{l=0}^{k-1} c_{ml} L_{lj}^{(1-\kappa)} R_j(t), \tag{4.3}$$

$$\frac{\partial \Phi_{n,k}(x_m,t)}{\partial x} = \left(\frac{\partial r(x)}{\partial x}\right)_{x_m} + \sum_{i=-n}^{n}\sum_{j=0}^{k-1}\sum_{l=0}^{k-1} w_{im}^{(1)} c_{il} L_{lj} R_j(t), \tag{4.4}$$

$$\frac{\partial^2 \Phi_{n,k}(x_m,t)}{\partial x^2} = \left(\frac{\partial^2 r(x)}{\partial x^2}\right)_{x_m} + \sum_{i=-n}^{n}\sum_{j=0}^{k-1}\sum_{l=0}^{n-1} w_{im}^{(2)} c_{il} L_{lj} R_j(t), \tag{4.5}$$

where

$$\begin{aligned} &L_{lj} = L_{k\times k}[l,j],\\ &L_{lj}^{(1-\kappa)} = L_{k\times k}^{(1-\kappa)}[l,j],\\ &w_{im}^{(1)} = \psi'(x_m)\delta_{i,m}^{(1)},\\ &w_{im}^{(2)} = \psi''(x_m)\delta_{i,m}^{(1)} + (\psi'(x_m))^2\delta_{i,m}^{(2)}. \end{aligned} \tag{4.6}$$

But for proof, according to the equations (1.2),(2.14),(2.28),(4.1) and (4.7) we get:

$$\int_0^t \frac{\partial \Phi(x,t)}{\partial t} dt = \Phi(x,t) - r(x), \tag{4.7}$$

$$\begin{aligned} \Phi_{n,k}(x_m,t) &= r(x_m) + \int_0^t \left(\sum_{i=-n}^{n}\sum_{j=0}^{k-1} c_{ij} S_i(x_m) R_j(t)\right) dt \\ &= r(x_m) + \sum_{j=0}^{k-1}\sum_{l=0}^{k-1} c_{ml} L_{lj} R_j(t). \end{aligned} \tag{4.8}$$

Also according to equations (2.17),(2.28),(4.1) and (4.8) we have:

$$\begin{aligned} \frac{\partial^\kappa \Phi_{n,k}(x_m,t)}{\partial t^\kappa} &= \left(D_t^\kappa r(x)\right)_{x_m} + \sum_{i=-n}^{n}\sum_{j=0}^{k-1}\sum_{l=0}^{k-1} c_{il} L_{lj}^{(1-\kappa)} S_i(x_m) R_j(t) \\ &= \left(D_t^\kappa r(x)\right)_{x_m} + \sum_{j=0}^{k-1}\sum_{l=0}^{k-1} c_{ml} L_{lj}^{(1-\kappa)} R_j(t). \end{aligned} \tag{4.9}$$

Next by using equations(2.29),(4.1) and (4.8) we get:

$$\begin{aligned}\frac{\partial\Phi_{n,k}(x_m,t)}{\partial x} &= \left(\frac{\partial r(x)}{\partial x}\right)_{x_m} + \sum_{i=-n}^{n}\sum_{j=0}^{k-1}\sum_{l=0}^{k-1} c_{il}L_{lj}\left(\frac{dS_i(x)}{dx}\right)_{x=x_m} R_j(t)\\ &= \left(\frac{\partial r(x)}{\partial x}\right)_{x_m} + \sum_{i=-n}^{n}\sum_{j=0}^{k-1}\sum_{l=0}^{k-1} c_{il}L_{lj}\left(\psi'(x)\frac{d}{d\phi}S_i(x)\right)_{x=x_m} R_j(t)\\ &= \left(\frac{\partial r(x)}{\partial x}\right)_{x_m} + \sum_{i=-n}^{n}\sum_{j=0}^{k-1}\sum_{l=0}^{k-1} c_{il}L_{lj}\left(\psi'(x_m)\delta_{i,m}^{(1)}\right) R_j(t). \end{aligned} \tag{4.10}$$

Finally according to equations(2.30),(4.1) and (4.8) we have:

$$\begin{aligned}&\frac{\partial^2\Phi_{n,k}(x_m,t)}{\partial x^2} = \left(\frac{\partial^2 r(x)}{\partial x^2}\right)_{x_m} + \sum_{i=-n}^{n}\sum_{j=0}^{k-1}\sum_{l=0}^{k-1} c_{il}L_{lj}\left(\frac{d^2S_i(x)}{dx^2}\right)_{x=x_m} R_j(t)\\ &= \left(\frac{\partial^2 r(x)}{\partial x^2}\right)_{x_m} + \sum_{i=-n}^{n}\sum_{j=0}^{k-1}\sum_{l=0}^{k-1} c_{il}L_{lj}\left(\psi''(x)\frac{d}{d\phi}S_i(x) + (\psi'(x))^2\frac{d}{d\phi^2}S_i(x)\right)_{x=x_m} R_j(t)\\ &= \left(\frac{\partial^2 r(x)}{\partial x^2}\right)_{x_m} + \sum_{i=-n}^{n}\sum_{j=0}^{k-1}\sum_{l=0}^{k-1} c_{il}L_{lj}\left(\psi''(x_m)\delta_{i,m}^{(1)} + (\psi'(x_m))^2\delta_{i,k}^{(2)}\right) R_j(t). \end{aligned} \tag{4.11}$$

In the following, using the above equations, the residual function $R_{n,k}(x_m,t)$ for equation(1.1) can be obtained as follows:

$$R_{n,k}(x_m,t) = \frac{\partial^\kappa\Phi_{n,k}(x_m,t)}{\partial t^\kappa} + \Phi_{n,k}(x_m,t)\frac{\partial\Phi_{n,k}(x_m,t)}{\partial x} - \gamma\frac{\partial^2\Phi_{n,k}(x_m,t)}{\partial x^2} - Q(x_m,t) \tag{4.12}$$

In order to approximate the function $\Phi(x,t)$, we must obtain the unknown coefficients $\{c_{ij}\}_{i=-n\ldots n}^{j=0\ldots k-1}$. For this purpose, we must equalize the $R_{n,k}(x,t)$ to zero at Haar and Sinc collocation points:

$$\begin{aligned}&R_{n,k}(x_m,t_i) = 0, \quad m=-n,...,n \quad ,i=1,2,...,k,\\ &x_m = \psi^{-1}(mh) = \frac{e^{mh}}{1+e^{mh}}, \quad m=0,\pm1,\pm2,...,\pm n\\ &t_i = \frac{2i-1}{2k}, \quad i=1,2,...,k. \end{aligned} \tag{4.13}$$

Eq. (4.13) gives a system of algebraic equations, and after solving the system with Maple software, the numerical results of the problem is obtained.

5 Numerical results and discussion

In this part, by giving 2 examples and calculating error norm and convergence rate below, we show that the accuracy and speed of the proposed algorithm is higher compared to the methods mentioned in

references [6],[1],[27] .

$$L^{\infty}-error=Max|\Phi^{*}(x_m,t_i)-\Phi(x_m,t_i)|_{m=-n}^{m=n},\quad t_i=\frac{2i-1}{2k},\quad i=1,2,...,k,$$
$$L^{2}-error=\sqrt{\frac{\sum_{m=-n}^{n}\left(\Phi^{*}(x_m,t_i)-\Phi(x_m,t_i)\right)^2}{2n+1}},\quad t_i=\frac{2i-1}{2k},\quad i=1,2,...,k,$$
$$C-rate=\frac{\log(\frac{e_{n_2,k}}{e_{n_1,k}})}{\log(\frac{h2}{h1})}.$$

where $\Phi^{*}(x_m,t_i),\Phi(x_m,t_i)$ are the exact and numerical approximation of Burgers' equation at points x_m,t_i respectively. Also, $e_{n_1,k},e_{n_2,k}$ are the errors corresponding to $h1=\frac{\pi}{\sqrt{2n_1}}$ and $h2=\frac{\pi}{\sqrt{2n_2}}$ respectively.

Example 1. First, we solve the following time-fractional Burgers' equation which its exact solution is $e^{x}t^{2}$ [1]:

$$\frac{\partial^{\kappa}\Phi(x,t)}{\partial t^{\kappa}}+\Phi(x,t)\frac{\partial\Phi(x,t)}{\partial x}-\gamma\frac{\partial^{2}\Phi(x,t)}{\partial x^{2}}=t^{4}e^{2x}-\gamma t^{2}e^{x}+\frac{2t^{2-\kappa}e^{x}}{\Gamma(3-\kappa)},$$
$$\Phi(x,0)=0,x\in[0,1],$$
$$\Phi(0,t)=t^{2},\Phi(1,t)=et^{2},t\in(0,1].$$

Table 1,2 show the L^{∞}-error,L^{2}-error and the convergence rates for $k=16$ and several values of n with the fractional parameter $\kappa=0.1,0.6,0.9$ and the $\gamma=1$. According to the tables 1,2, we can see that with the increase of the number of collocation points(n), the convergence order of the algorithm also increases. Also, the speed of convergence is generally higher for κ values that close to 0 and 1 than the middle values. Figure 1 shows the logarithmic scale mode of L^{∞}-error and L^{2}-error for $\kappa=1$ and $k=16,\gamma=1$ for different values of n. According to the figure, we can see that the values of L^{2}-error are lower than those of L^{∞} for the same values of n.
Also, since in this semi-log representation the error variations are approximately linear versus n, we observe that the values of error decay exponentially and we can conclude that the convergence rate of the proposed method is exponential rate.

Example 2. Next, we solve following Burgers' equation which its exact solution is $\left(5e^{-\left(\frac{x}{2}+\frac{t^{\kappa}}{4\Gamma(1+\kappa)}\right)}-1\right)^{-1}$ [6]:

$$\frac{\partial^{\kappa}\Phi(x,t)}{\partial t^{\kappa}}+\Phi(x,t)\frac{\partial\Phi(x,t)}{\partial x}-\gamma\frac{\partial^{2}\Phi(x,t)}{\partial x^{2}}=0,$$
$$\Phi(x,0)=\frac{1}{\left(5\cosh\frac{x}{2}-\sinh\frac{x}{2}-1\right)},x\in[0,1],$$
$$\Phi(0,t)=\frac{1}{5e^{-\frac{t^{\kappa}}{4\Gamma(1+\kappa)}}-1},\Phi(1,t)=\frac{1}{5e^{-(0.5+\frac{t^{\kappa}}{4\Gamma(1+\kappa)})}-1},t\in(0,1].$$

Table 3 shows the comparison of numerical solution $\Phi(x,0.02)$ and absolute errors obtained by our method for $n=17,k=32$ and $\gamma=1,\kappa=0.8$ with finite integration method-shifted Chebyshev polynomials (FIM-SCP) in [6] and the expansion method with Cole–Hopf transformation (EPM-CHT) in [27]. According to these values, we find that the numerical results of our method are more accurate.
Figure 2 shows the surface plot of $\Phi(x,t)$ obtained by proposed method for $\kappa=1,n=17,k=16$ and $\gamma=1$.

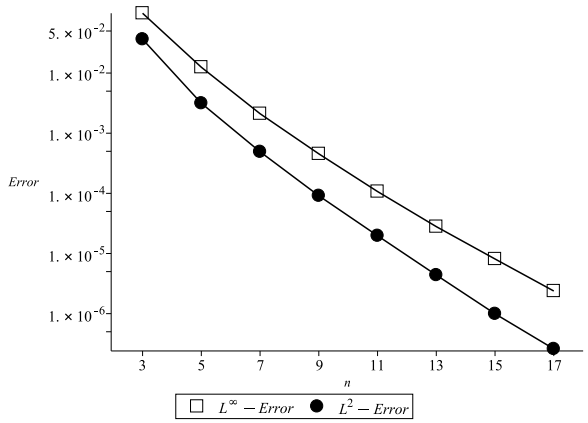

Figure 1: Logarithmic scale of L^∞-error and L^2-error for Example 1 ($\kappa = 1$, $k = 16$,$\gamma = 1$) for different values of n .

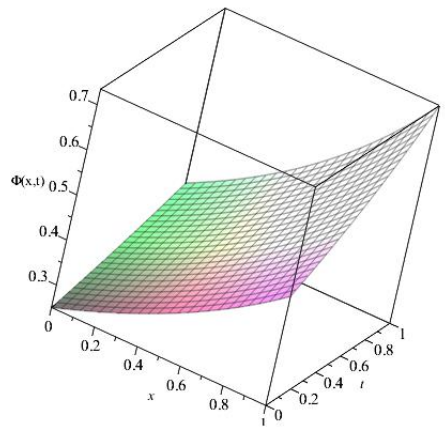

Figure 2: Surface plot of $\Phi(x, t)$ obtained by proposed method for Example 2 ($\kappa = 1, n = 17, k =$ 16, $\gamma = 1$)

Table 1: Numerical results of L^∞-error and C-rate for $k = 16, \gamma = 1$, for Example 1.

		$\alpha = 0.1$		$\alpha = 0.6$		$\alpha = 0.9$	
n	$h = \frac{\pi}{\sqrt{2n}}$	L^∞-error	C-rate	L^∞-error	C-rate	L^∞-error	C-rate
3	1.283e00	1.240e-01	-	1.621e-01	-	1.327e-01	-
5	9.935e-01	3.487e-02	4.961	6.422e-02	3.627	3.791e-02	4.906
7	8.400e-01	1.214e-02	6.286	2.580e-02	5.420	1.180e-02	6.938
9	7.406e-01	4.815e-03	7.354	1.085e-02	6.893	4.521e-03	7.634
11	6.699e-01	1.942e-03	9.040	5.374e-03	7.003	1.805e-03	9.151
13	6.161e-01	7.872e-04	10.786	2.917e-03	7.315	7.387e-04	10.697
15	5.736e-01	3.582e-04	11.016	1.552e-03	8.818	3.210e-04	11.647
17	5.388e-01	1.432e-04	14.649	8.371e-04	9.865	1.401e-04	13.260

Table 2: Numerical results of L^2-error and C-rate for $k = 16, \gamma = 1$, for $k = 16, \gamma = 1$, for Example 1.

		$\alpha = 0.1$		$\alpha = 0.6$		$\alpha = 0.9$	
n	$h = \frac{\pi}{\sqrt{2n}}$	L^2-error	C-rate	L^2-error	C-rate	L^2-error	C-rate
3	1.283e00	1.321e-01	-	1.425e-01	-	1.258e-01	-
5	9.935e-01	3.357e-02	5.364	4.123e-02	4.853	3.378e-02	5.149
7	8.400e-01	9.102e-03	7.758	1.395e-02	6.440	8.920e-03	7.915
9	7.406e-01	2.570e-03	10.063	5.410e-03	7.544	2.611e-03	9.777
11	6.699e-01	8.452e-04	11.083	2.218e-03	8.883	8.821e-04	10.815
13	6.161e-01	2.824e-04	13.125	1.015e-03	9.350	2.762e-04	13.902
15	5.736e-01	9.261e-05	15.580	4.631e-04	10.969	8.954e-05	15.741
17	5.388e-01	3.127e-05	17.350	1.992e-04	13.478	2.964e-05	17.667

6 Conclusion

Nonlinear time fractional Burgers' equation, which is one of the most important equation in the field of physics and fluid mechanics have been solved numericaly by Haar-Sinc collocation method. The time part of this equation, which is expressed as fractional derivatives, is discretized by Haar operational matrix of the fractional order, and the space part of the equation is discretized with the orthogonal Sinc functions. According to the data mentioned in the tables and figures, it can be said that the accuracy and convergence rate of the method increases exponentially with the increase of collocation points. It can also be seen that the accuracy of the algorithm increases as the Caputo's fractional derivative (κ) tend zero and one. Also we can see that generally the values of L^2-error are lower than those of L^∞ for the same values of collocation points number.

References

[1] I. Ali, S. Haq, S.F. Aldosary, K.S. Nisar, F. Ahmad, Numerical solution of one- and twodimensional time-fractional burgers equation via lucas polynomials coupled with finite difference method, Alexandria Engineering Journal, 61, 2022, 6077-6087.

Table 3: Absolute errors obtained by present method for $n = 17, k = 32$ and $\kappa = 0.8, \gamma = 1$ for Example 2.

	FIM-SCP[6]		EPM-CHT[27]		Our Algorithm	
x	$\Phi(x, 0.02)$	Error	$\Phi(x, 0.02)$	Error	$\Phi(x, 0.02)$	Error
0.02	0.256913	6.7146e-06	0.256321	5.84566e-04	0.256903	7.1573e-07
0.04	0.260173	1.3390e-05	0.259566	5.93809e-04	0.260160	8.7624e-07
0.06	0.263483	2.0005e-05	0.262860	6.03243e-04	0.263458	6.2547e-06
0.08	0.266844	2.6539e-05	0.266204	6.12874e-04	0.266808	9.2461e-06
0.10	0.270256	3.2970e-05	0.269601	6.22707e-04	0.270211	1.0579e-05

[2] J.M. Burgers, A Mathematical Model Illustrating the Theory of Turbulence, Adv. Appl. Mech. Academic Press, New York, 1948.

[3] C.F. Chen, C. Hsiao, Haar wavelet method for solving lumped and distributed-parameter systems, IEEE. Proc. Cont.Theo. Appl., 144 1997, 87-94.

[4] L. Chen, S. Lu, T. Xu, Fourier spectral approximation for time fractional burgers equation with non smooth solutions, Applied Numerical Mathematics, 169 2021, 164-178.

[5] Y. Chen, M. Yi, C. Yu, Error analysis for numerical solution of fractional differential equation by Haar wavelets method, J. Comput. Sci., 3 2012, 367-373.

[6] A. Duangpan, R. Boonklurb, and T. Treeyaprasert, Finite integration method with shifted chebyshev polynomials for solving time-fractional burgers' equations, Mathematics, 7(12) 2019, 1201.

[7] M.S. Hashmi, M. Wajiha, S.W. Yao, A. Ghaffar, M. Inc, Cubic spline based differential quadrature method: A numerical approach for fractional burger equation, Results in Physics, 26(3) 2021, 104415.

[8] M.H. Heydari, Z. Avazzadeh, A. Atangana, Orthonormal shifted discrete legendre polynomials for solving a coupled system of nonlinear variable-order time fractional reaction-advection-diffusion equations, Applied Numerical Mathematics, 161 2021, 425-436.

[9] M.H. Heydari, Z. Avazzadeh, N. Hosseinzadeh, Haar wavelet method for solving high-order differential equations with multi-point boundary conditions, Journal of Applied and Computational Mechanics, 8(2) 2022, 528-544.

[10] M. Hussain, S. Haq, Weighted meshless spectral method for the solutions of multi-term time fractional advection-diffusion problems arising in heat and mass transfer, Int. J. Heat Mass Transf., 129, 2019, 1305-1316.

[11] M. Hussain, S. Haq, A. Ghafoor, I. Ali, Numerical solutions of time-fractional coupled viscous burgers' equations using meshfree spectral method, Comput. Appl. Math., 39(1) 2020, 6.

[12] M. Kashif, K. D. Dwivedi, T. Som, Numerical solution of coupled type fractional order burgers equation using finite difference and fibonacci collocation method, Chinese Journal of Physics, 77 2022, 2314-2323.

[13] A.A. Kilbas, H. Srivastava, J. Trujillo, A Mathematical Model Illustrating the Theory of Turbulence. San Diego: Elsevier, 2006.

[14] C. Li, D. Li, Z. Wang, L1/ldg method for the generalized time-fractional burgers equation, Mathematics and Computers in Simulation, 187 2021, 357-378.

[15] Y. Li, W. Zhao, Haar wavelet operational matrix of fractional order integration and its applications in solving the fractional order differential equations, Appl. Math. Comput., 216, 2010, 2276-2285.

[16] J. Lund, K. Bowers, Sinc methods for quadrature and differential equations. SIAM, Philadelphia, 1992.

[17] M. Onal, A. Esen, A crank-nicolson approximation for the time fractional burgers equation, Appl. Math. Nonlin. Sci., 5(2) 2020, 177-184.

[18] O. Oruc, A. Esen, F. Bulut, A unified finite difference chebyshev wavelet method for numerically solving time fractional burgers' equation, Disc. Cont. Dyn. Syst., 12(3) 2019, 533-542.

[19] K. Parand, M. Dehghan, A. Pirkhedri, Sinc-collocation method for solving the blasius equation, Phy. Let. A., 373(4) 2009, 4060-4065.

[20] K. Parand, M. Dehghan, A. Pirkhedri, The Sinc-collocation method for solving the thomas-fermi equation, Appl. Math. Comput., 237(1) 2013, 244-252 .

[21] A. Pirkhedri ,H.H. S. Javadi, Solving the time-fractional diffusion equation via Sinc–Haar collocation method, Applied Mathematics and Computation, 257 2015, 317-325.

[22] M. Razzaghi, Y. Ordokhani, Solution of differential equations via rationalized Haar functions, Math. Comput. Simul., 56 2001, 235-246.

[23] B. K. Singh, M. Gupta, Trigonometric tension b-spline collocation approximations for time fractional burgers' equation, Journal of Ocean Engineering and Science, In Press, 2022.

[24] F. Stenger, Integration formulas via the trapezoidal formula, J. Inst. Math. App., 12 1973, 103-114.

[25] V.K. Tamboli, P.V. Tandel, Solution of the time-fractional generalized burger–fisher equation using the fractional reduced differential transform method, Journal of Ocean Engineering and Science, 7(4) 2022, 399-407.

[26] D. Tavares, R. Almeida, D.F. Torres, Caputo derivatives of fractional variable order: Numerical approximations, communications in nonlinear science and numerical simulation, 35 2016, 69-87.

[27] A. Yokus, D. Kaya, Numerical and exact solutions for time fractional burgers equation, J. Nonlinear Sci. Appl, 10 2017, 3419-3428.